ELSEVIER

Polymer 42 (2001) 3761–3769

polymer

www.elsevier.nl/locate/polymer

Fluorine incorporation in plasma-polymerized octofluorocyclobutane, hexafluoropropylene and trifluoroethylene

L. Sandrin[a], M.S. Silverstein[b,*], E. Sacher[c]

[a]*Laboratoire Ondes et Acoustique, ESPCI, 75005 Paris, France*
[b]*Department of Materials Engineering, Technion — Israel Institute of Technology, Haifa 32000, Israel*
[c]*Département de Génie Physique et de Génie de Matériaux, École Polytechnique de Montréal, C.P. 6079, Succursale C-V, Montréal, Que., Canada H3C 3A7*

Received 9 May 2000; received in revised form 14 August 2000; accepted 15 August 2000

Abstract

The need for increased signal transmission speed and device density in the next generation of multilevel integrated circuits (ICs) places stringent demands on materials performance. There is a requirement for interlayer dielectrics with permittivities under 3 (low κ dielectrics) that have compatibility with copper and copper processing. Plasma polymerization is a solvent-free, room temperature process that can be used to rapidly deposit thin polymer films on a wide variety of substrates. This paper describes the deposition of plasma polymers from several fluorinated monomers (octofluorocyclobutane (OFCB), hexafluoropropylene (HFP) and trifluoroethylene (TrFE)), and evaluates their molecular structures. Films with relatively high F/C ratios were investigated in detail. The refractive index, n, of plasma-polymerized OFCB (PPOFCB), 1.37 at a wavelength of 900 nm, indicates that it has a high frequency permittivity (n^2) of about 2.0. The plasma fluoropolymers were transparent, yellow films that adhered strongly to the substrates and were deposited at constant deposition rates that ranged from 0.03 μm/min for PPOFCB to 0.34 μm/min for PPHFP. The AFM-determined roughness of PPOFCB on copper is 0.46 nm, half the 0.97 nm roughness of the substrate. The significantly rougher PPTrFE and PPHFP consist of spherical particles from predominantly gas phase polymerizations. The incorporation of fluorine in the polymer is greater and more efficient for PPOFCB and PPHFP than for PPTrFE. For PPOFCB, F/C increases with decreasing W/F_m (where W is the plasma power and F_m is the mass flow rate) and, in a less sensitive manner, with increasing pressure. A typical PPOFCB has an F/C of approximately 1.5 and approximately 1.5% oxygen resulting from the reaction of long lived radicals in the plasma polymer with atmospheric oxygen. PPOFCB and PPHFP have similar molecular structures, consisting of random assemblies of fluorinated carbon groups. CF_2 groups are more prevalent in PPOFCB, reflecting the monomer structure and the low W/F_m. CF groups and unsaturation are more prevalent in PPHFP, reflecting the monomer structure and the high W/F_m. © 2001 Elsevier Science Ltd. All rights reserved.

Keywords: Plasma polymerization; Fluoropolymer; Low κ dielectric

1. Introduction

The demand for increased signal transmission speed and device density in the next generation of multilevel integrated circuits (ICs) places stringent demands on materials performance. Higher packing density requires a large increase in the number of interconnects and this has led to an increase in the number of wiring levels and a reduction in wiring pitch (sum of metal line width and between-line spacing) to increase the wiring density. As device dimensions are already below 0.25 μm (transistor gate length), properties such as propagation delay, crosstalk noise and power dissipation due to resistance–capacitance (RC) coupling become significant with increases in the metal line resistance and the line-to-line capacitance of the interlayer dielectrics (ILD) [1]. The interconnect delay becomes the major fraction of the total delay and limits the improvement in device performance.

The 'National Technology Roadmap for Semiconductors (NTRS) — Technology Needs', released by the Semiconductor Manufacturing Technology Consortium (SEMATECH) and sponsored by the Semiconductor Industry Association (SIA), has defined two critical changes needed for the development of ultra large scale integrated circuits (ULSI): the reduction of resistance (R) and the reduction of capacitance (C). The NTRS has charted the present and future needs ILD [2]. The current need is for a permittivity less than 3. A suitable low permittivity material (low κ dielectric) for near future needs has yet to be found because, according to NTRS, 'materials that simultaneously meet the electrical, mechanical and thermal requirements have been

* Corresponding author. Tel.: +972-4-829-4582, fax: +972-4-832-1978.
E-mail address: michaels@tx.technion.ac.il (M.S. Silverstein).

0032-3861/01/$ - see front matter © 2001 Elsevier Science Ltd. All rights reserved.
PII: S0032-3861(00)00693-5

elusive'. Fluoropolymers have low permittivities but are difficult to process. The authors have investigated fluoropolymer sputtering, spin-cast perfluorinated dioxole polymers, and plasma polymerization in an attempt to produce thin fluoropolymer films [3–11].

Plasma polymerization is a solvent-free, room temperature process that can be used to rapidly deposit thin polymer films onto a wide variety of substrates [12,13]. In plasma polymerization, a neutral 'monomer' gas or vapor in a low pressure reactor is subjected to an electric field. The monomer is fragmented into reactive species, which subsequently recombine, forming a crosslinked polymer. The 'monomer' can be a hydrocarbon, fluorocarbon, organosilicon or organometallic and need not necessarily include the functional groups typically associated with conventional polymerization techniques [12]. The molecular structure and properties of the plasma polymer depend on the monomer, plasma power, monomer flow rate and reactor pressure. The advantages of plasma polymerization include: the environmental friendliness of the solvent-free process; the deposition of ultra-thin films with thickness directly proportional to deposition time; the deposition of pinhole-free films without the dimensional changes associated with solvent evaporation; the deposition of highly adherent films with substrate activation in the plasma environment; the plethora of monomers available; and the simplicity of the reactor (standard microelectronics industry plasma cleaning equipment). This paper will describe the deposition of plasma polymers from several fluorinated monomers and evaluate their molecular structures. A subsequent paper will describe the interaction of plasma-polymerized octafluorocyclobutane with a copper substrate during the deposition process [14].

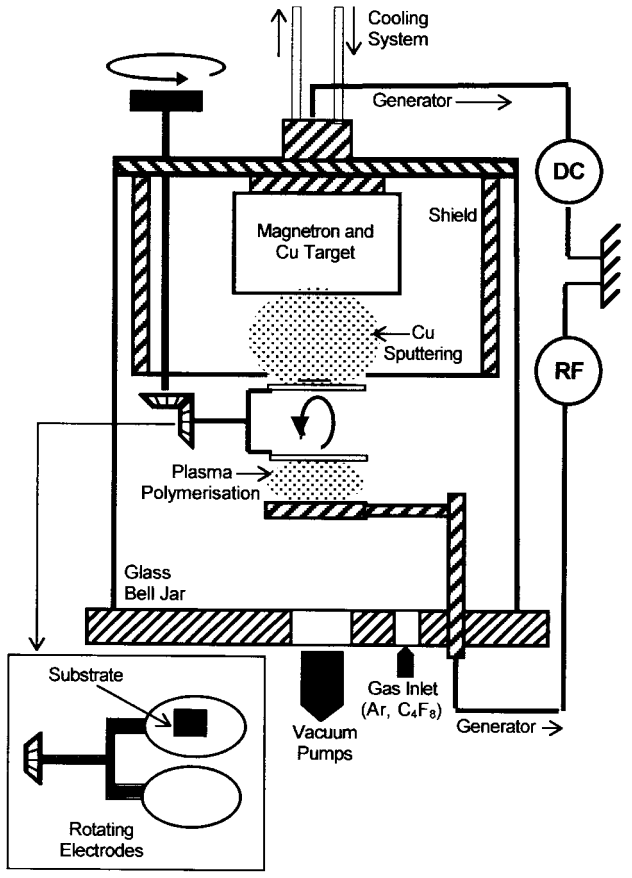

Fig. 1. Schematic diagram illustrating Cu sputtering/plasma polymerization chamber.

2. Experimental

2.1. Materials

The fluorocarbon monomers (Matheson) used for plasma polymerization (PP) were octafluorocyclobutane (OFCB, C_4F_8), trifluoroethylene (TrFE, C_2F_3H) and hexafluoropropylene (HFP, C_3F_6). The substrates used were silicon wafers, glass slides, polyethylene (PE) films, or NaCl single crystals. The PPOFCB and PPTrFE polymerizations and characterizations were carried out at the Department of Engineering Physics, Ecole Polytechnique, while the PPHFP polymerization and characterization were carried out at the Department of Materials Engineering, Technion. A description of the PPOFCB and PPTrFE depositions will be followed by a description of the PPHFP deposition.

2.2. Plasma polymerization

The copper sputtering and PPOFCB and PPTrFE plasma polymerization were carried out using the innovative reactor illustrated schematically in Fig. 1. A unique feature of this reactor is the specimen stage for copper sputtering which, when rotated, became the upper parallel-plate electrode for plasma polymerization. In this manner, a plasma polymer could be deposited on sputter-coated copper without breaking vacuum. The chamber could be evacuated to 10^{-8} Pa (base pressure) and the operating pressure was regulated independently of the gas flow, using a Baratron valve. The gas flow rates were controlled using mass flow controllers. An RF generator (13.56 MHz) and matching unit were used for plasma polymerization and a DC magnetron generator was used to sputter copper.

The substrate was placed on the specimen stage. The stage was rotated such that the substrate was positioned on the upper parallel-plate plasma electrode. The substrate was cleaned in an argon plasma (10 sccm, 67 Pa, 50 W) for 2 min and then the chamber was evacuated to base pressure. The stage was rotated 180° such that the substrate was positioned beneath the copper target. The substrate was coated with sputtered copper at 0.1 μm/min (0.5 A, 360 V) for 3 min in an argon atmosphere (2.7 Pa, 5 sccm) and then the chamber was evacuated to base pressure. The stage was rotated 180° such that the copper-coated substrate was again positioned as the upper parallel-plate plasma electrode. Plasma polymerization was then carried out at

powers ranging from 5 to 50 W, pressures from 2.7 to 40 Pa, and flow rates from 10 to 24 sccm. Typical conditions for OFCB were 7 W, 33 Pa, 24 sccm.

The PPHFP polymerization was carried out in a commercial parallel-plate electrode radio frequency (13.56 MHz) plasma reactor (Jupiter III, March Instruments) that has been described in detail elsewhere [8]. The reactor could be evacuated to 2.5 Pa with a vacuum pump (AC-2012, Alcatel) and the temperature of the anodized aluminum parallel-plate electrodes was maintained at 20°C with a circulating liquid cooler (RTE-100, Neslab). The substrates were centered on the bottom electrode, the reactor was evacuated to 2.5 Pa, the substrate was cleaned with an argon plasma (200 W, 100 Pa, and 16.9 sccm) for 5 min before the reactor was again evacuated to 2.5 Pa prior to plasma polymerization. The molar flow rate of HFP and the total pressure in the reactor were kept constant (18.3 sccm and 187 Pa, respectively) and powers of 25–250 W were used, with a typical power of 100 W.

2.3. Thickness and permittivity

The thicknesses of the PPOFCB and PPTrFE films were measured using both a profilometer (model 3030ST, Dektak) and a variable angle spectroscopic ellipsometer (model 200, J.A. Woollam) in reflection. The ellipsometer was also used to characterize the refractive index, n, as a function of wavelength. The permittivity, κ, was taken as n^2. The thicknesses of the PPHFP films were measured using a profilometer with an accuracy of 0.05 μm (α-Step100, Tencor).

2.4. Molecular structure and topography

The molecular structure was characterized using a combination of X-ray photoelectron spectroscopy (XPS) and Fourier transform infrared spectroscopy (FTIR). For PPOFCB and PPTrFE, XPS analysis was carried out using a non-monochromated MgK_α source (ESCALAB MKII, Vacuum Generators). For PPHFP an Al K_α source XPS was used (Perkin–Elmer, Physical Electronics 555 ESCA/Auger). Both low-resolution survey and high-resolution core level spectra were taken for carbon, fluorine and oxygen. Elemental concentrations were evaluated from the high resolution peak areas following Shirley background subtraction [15]. PPOFCB was deposited on NaCl single crystals for FTIR characterization (RS, Mattson). The PPHFP films for FTIR characterization (1000, Mattson) were separated from glass substrates by soaking in acetone.

The PPOFCB and PPTrFE topographies were characterized using atomic force microscopy (AFM) in contact mode (model 2010, Topometrix). Scans of 5×5, 1×1 and 0.2×0.2 μm^2 were conducted at 20, 5 and 1 μm/s, respectively. The roughness was obtained from the 0.2×0.2 μm^2 scan. The PPHFP topography was characterized using scanning electron microscopy (SEM) (JEOL JSM-840) after coating the film with 0.05 μm of evaporated gold.

2.5. Adhesion

Micro-scratch tests were performed to measure adhesion of PPOFCB to copper (CSEM Microscratch Tester, MST). An 0.8 mm radius hemispherical diamond indentor was placed on the sample surface, the sample was moved under the indentor at a constant speed of 0.5 mm/min, and a linearly increasing normal force ramp, in the range 0–3 N, was applied. The indentor-sample interaction was recorded on video tape and the adhesion was calculated from the normal force at which film-substrate debonding began.

3. Results and discussion

3.1. Deposition rate

The plasma polymer films discussed here were all transparent and yellow. Plasma polymer deposition rates are generally relatively independent of polymerization time. A linear increase in thickness with time is observed for a typical PPOFCB (7 W, 24 sccm, 33.3 Pa), as shown in Fig. 2. Similar linear behavior is seen in Fig. 2 for a typical PPHFP (100 W, 18.3 sccm, 187 Pa). The deposition rates calculated from Fig. 2 are 0.03 μm/min for PPOFCB and 0.34 μm/min for PPHFP. The significantly higher deposition rate for PPHFP reflects the higher plasma power that enhances monomer fragmentation, the higher reactor pressure that increases the concentration of reactive species and the double bond in HFP that may enhance reactivity. The deposition rate for PPTrFE, polymerized under conditions similar to those of PPOFCB, was significantly higher than that of PPOFCB. The higher deposition rates under similar polymerization conditions reflect the influence of the double bond as well as that of hydrogen present in the monomer: hydrogen scavenges fluorine radicals through the formation of HF, reducing the extent of etching [9].

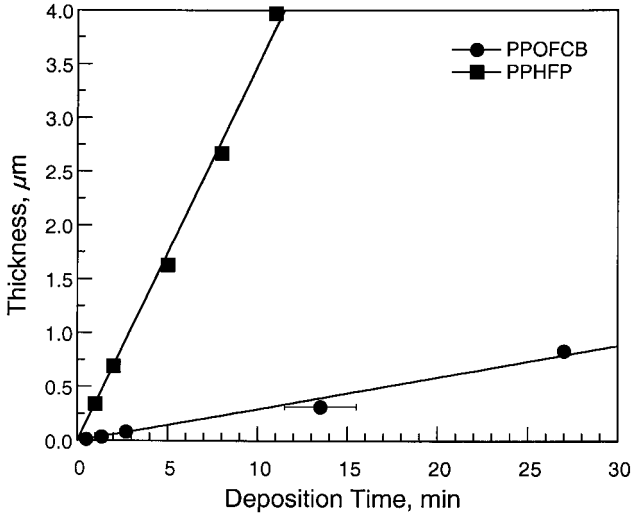

Fig. 2. Thickness as a function of deposition time for PPOFCB (7 W, 24 sccm, 33.3 Pa) and PPHFP (100 W, 18.3 sccm, 187 Pa).

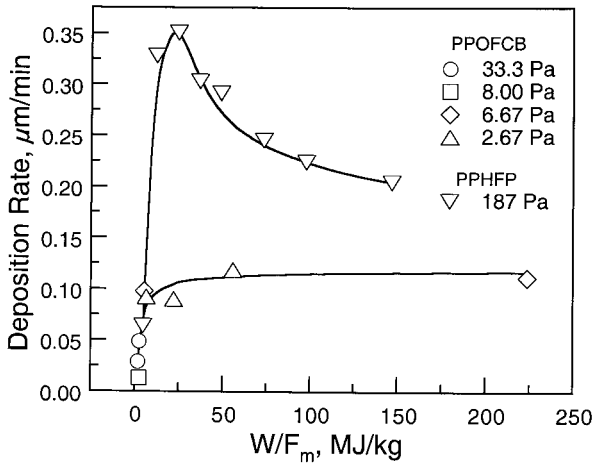

Fig. 3. Deposition rate as a function of W/F_m for various monomers and pressures. PPOFCB: 33.3, 8.00, 6.67, 2.67 Pa. PPHFP: 187 Pa.

The variation of the PPOFCB deposition rate with W/F_m in Fig. 3 is typical of plasma polymerization. The low deposition rate at low W/F_m reflects deposition in an energy-poor plasma. The deposition rate increases with increasing energy per mass monomer until a plateau is reached at a critical W/F_m (approximately 25 MJ/kg). The reaction is energy saturated beyond this critical value and the deposition rate does not increase further. The PPHFP deposition rate in Fig. 3 reaches a maximum at approximately the same critical value, 25 MJ/kg. This maximum deposition rate is three times that for PPOFCB, reflecting the higher reactor pressure and higher concentration of monomer as well as the presence of the double bond in HFP. The PPHFP deposition rate decreases with further increases in W/F_m. This decrease in the deposition rate reflects the increasing dominance of the plasma etching reaction typical of fluorocarbon plasmas. Based on the molecular structure of OFCB, fragmentation would tend to yield CF_2, which enhances polymerization [16]. Based on the molecular structure of HFP, fragmentation would tend to yield CF and CF_3, which enhance etching and would reduce the rate of deposition with increasing W/F_m [16].

3.2. Topography

There are significant differences in topography among micrometer thick plasma polymer films from different monomers deposited on glass in Fig. 4. PPOFCB (7 W, 2.67 Pa, 24 sccm), Fig. 4a, has a relatively smooth topography. To the naked eye, both PPTrFE and PPHFP seem to be homogeneous, transparent films. The PTrFE (7 W, 2.67 Pa, 10 sccm) and PPHFP (100 W, 18.3 sccm, 187 Pa) topographies revealed in Fig. 4b and c, respectively, are actually assemblies of submicrometer particles. The PPTrFE film is assembled from particles of about 100–200 nm in diameter while the PPHFP film is assembled from particles 200 to 500 nm in diameter, some of which

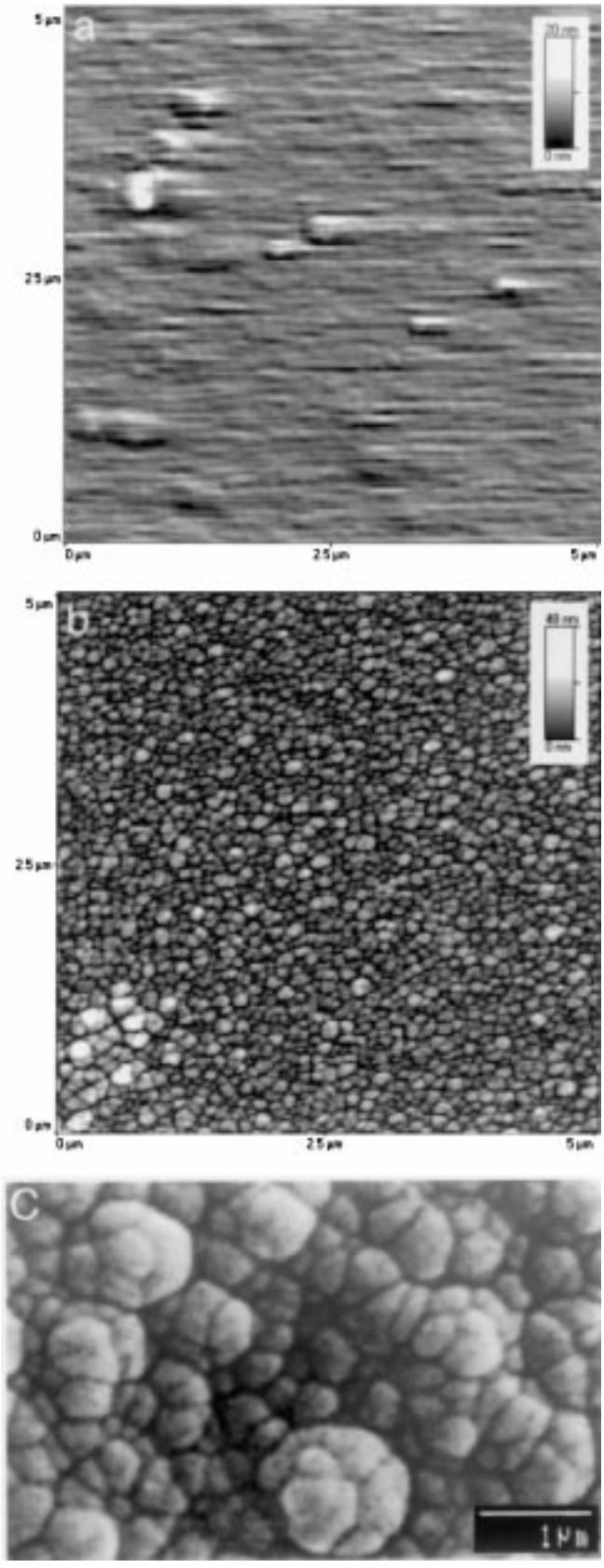

Fig. 4. Micrographs of 0.5 μm thick plasma polymer films: (a) PPOFCB (7 W, 24 sccm, 2.67 Pa), AFM; (b) PPTrFE (7 W, 10 sccm, 2.67 Pa), AFM; (c) PPHFP (100 W, 18 sccm, 187 Pa), SEM.

are organized in spherical clusters about 1 μm in diameter. The RMS roughness of a copper-sputtered silicon wafer, measured using AFM, was 0.97 nm. PPOFCB (7 W, 2.67 Pa, 24 sccm) deposited on the copper had a roughness of 0.46 nm, reflecting the smoothness of the surface in Fig. 4a. PPTrFE deposited on the copper under similar conditions (7 W, 2.67 Pa, 10 sccm) has a roughness of 2.3 nm, reflecting the particulate structure in Fig. 4b.

The smooth PPOFCB surface suggests that polymerization occurs predominantly on the substrate surface. The polymer film grows through reaction with the monomer fragments that reach the surface. This polymerization mechanism yields the relatively slow deposition rate seen in Fig. 2. The rough PPTrFE and PPHFP surfaces suggest that polymerization occurs predominantly in the gas phase, yielding the relatively rapid deposition rate seen in Fig. 2. Increasing the pressure enhances the tendency towards gas phase, as opposed to surface, polymerization. Spherical particles formed in the gas phase would then deposit on the surface [9]. PPOFCB films polymerized at higher pressures are still transparent and homogeneous to the naked eye but have a structure similar to that for PPHFP, in Fig. 4c. PPTrFE films polymerized at higher pressures became cloudy, indicating the beginning of powder formation and the incorporation of relatively large powder particles within the film. A loose powder, with particles tens to hundreds of micrometers in diameter, is deposited at even higher pressures.

3.3. Molecular structure

The atomic compositions in Table 1 represent typical plasma polymer films. PPOFCB (7 W, 2.67 Pa, 24 sccm) has an F/C of 1.53, and 1.2% oxygen, resulting from the reaction of long-lived radicals in the plasma polymer with atmospheric oxygen. The atomic composition and F/C of a typical PPHFP (100 W, 18.3 sccm, 187 Pa) in Table 1 are quite similar to those of PPOFCB. For PPOFCB and PPHFP, dividing the film F/C (about 1.5) by the monomer F/C (2) yields 0.75. For PPTrFE (7 W, 2.67 Pa, 24 sccm), dividing the film F/C (0.73) by the monomer F/C (1.5) yields 0.49, significantly lower than those for PPOFCB and PPHFP. Not only is there is less fluorine in PPTrFE but also the incorporation of fluorine from the monomer into the polymer is less efficient. This less efficient fluorine incorporation may be related to the presence of hydrogen in the monomer. The hydrogen released by monomer fragmentation scavenges fluorine, forming HF and, possibly, other fluorinated gaseous species that are removed by the vacuum and thus do not contribute to the polymer structure [9]. PPOFCB and PPHFP, with their relatively high F/C ratios, are of greater interest for low permittivity applications since the permittivity should decrease with increasing F/C.

Table 1
Atomic compositions of PPOFCB and HFP

Element	Atomic concentration (%)	
	PPOFCB	PPHFP
F	59.8	59.1
C	39.0	39.4
O	1.2	1.5
F/C	1.53	1.50

The F/C ratio of PPOFCB (Fig. 5) decreases with W/F_m and increases with pressure at low W/F_m. F/C is more sensitive to W/F_m than to pressure, with a 50% increase in W/F_m yielding a more significant change in F/C than a 50% increase in pressure.

The curve fits for plasma fluoropolymer C_{1s} spectra in the literature usually include CF_3, CF_2, CF and C^*–CF peaks and, in some cases, a CH peak [12,16]. There is no regular molecular structure in this random addition of monomer fragments and, therefore, the molecular environments of identical groups may be quite varied. This irregular molecular structure, therefore, yields especially broad binding energy peaks. Full widths at half maximum (FWHM) of 2 eV are common for plasma polymers [12]. The close proximity of numerous broad peaks in plasma fluoropolymers yields spectra whose interpretation can be especially challenging. An additional factor that must be taken into account in the interpretation of the spectra is the presence of $\alpha_{3,4}$ X-ray satellites [17]. The α_3 satellite, 8.0% of the main peak area, is located −8.4 eV from the main peak; the α_4 satellite, 4.2% of the main peak area, is located −10.2 eV from the main peak. CF_3 and CF_2, at 293.5 and 291.4 eV, respectively, will, therefore, have satellite contributions near the CH binding energy, 285 eV.

The binding energy peak positions were determined for the plasma polymerized fluorocarbons using the C_{1s} spectra in Fig. 6. PPOFCB films, approximately 15 nm thick, were deposited on both copper and PE. The film thickness was calibrated using depositions of PPOFCB on copper; the

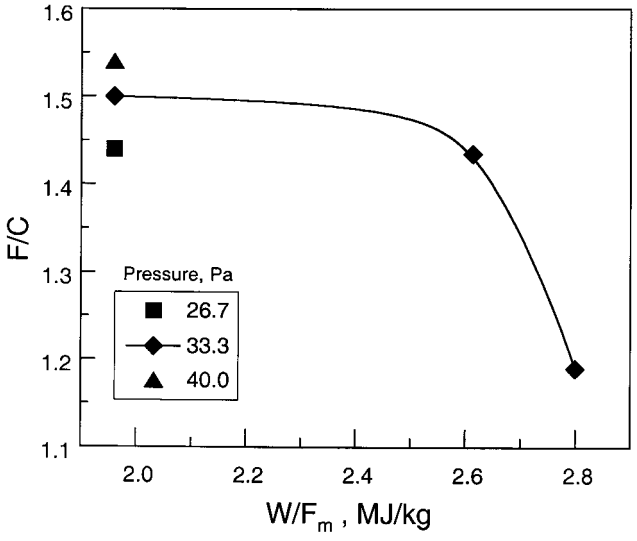

Fig. 5. F/C ratio as a function of W/F_m for PPOFCB at various pressures.

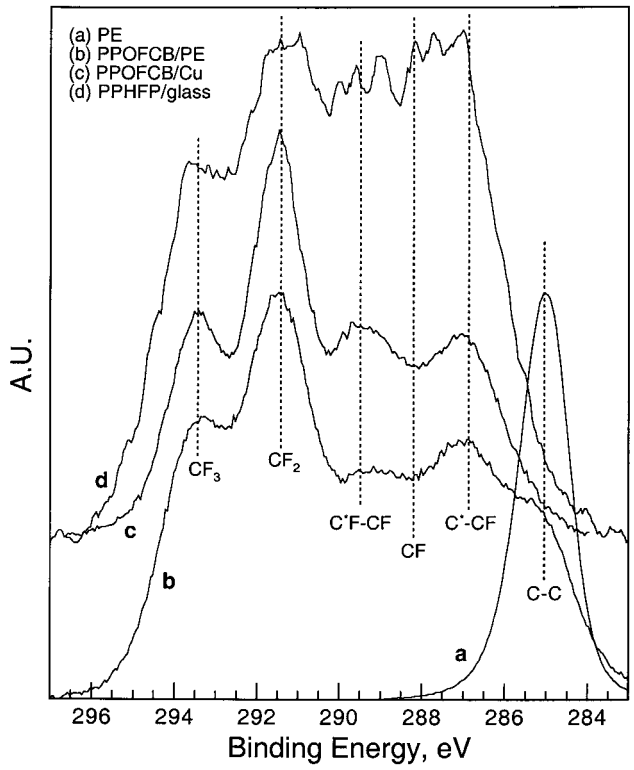

Fig. 6. C_{1s} spectra: (a) PE substrate; (b) 15 nm PPOFCB (7 W, 10 sccm, 2.67 Pa) on PE; (c) 15 nm PPOFCB (7 W, 10 sccm, 2.67 Pa) on Cu; and (d) PPHFP (100 W, 18 sccm, 187 Pa) on glass.

thickness of PPOFCB on PE may be less than the 15 nm found on copper. This film thickness is close to the penetration depths (3× the mean free paths) of the various photoemitted electrons. The C_{1s} photoelectrons originating in the PE substrate have a higher mean free path through the

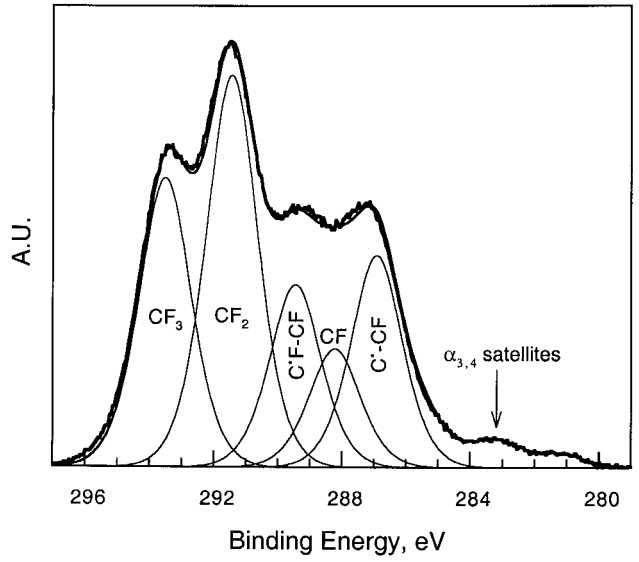

Fig. 7. C_{1s} spectrum curve fit for PPOFCB (7 W, 10 sccm, 2.67 Pa). Thick line: data. Thin lines: individual peaks and the sum of all peaks and satellites.

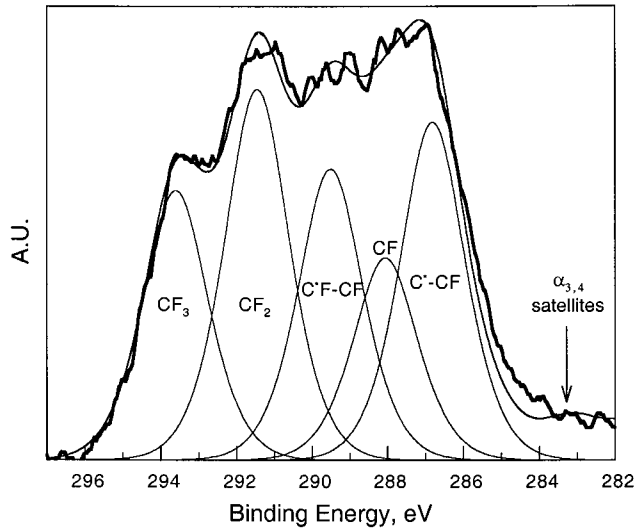

Fig. 8. C_{1s} spectrum curve fit for PPHFP (100 W, 18 sccm, 187 Pa). Thick line: data. Thin lines: individual peaks and the sum of all peaks and satellites.

PPOFCB than the Cu_{2p} photoelectrons from the copper substrate and, hence, it was possible to detect the substrate beneath the PPOFCB film. The C_{1s} spectrum of the PE substrate is seen in Fig. 6a; it has one peak, at 285 eV. The PPOFCB spectra are almost identical, whether on PE (Fig. 6b) or copper (Fig. 6c), the only difference between them being a shoulder at 285 eV in Fig. 6b for PE beneath the PPOFCB film. Using the peak at 285 eV as a reference, binding energies were assigned to other PPOFCB peaks. The peak at the highest binding energy, 293.6 eV, was assigned to CF_3. The peak with the second highest binding energy, 291.5 eV, (and the highest magnitude) was assigned to CF_2. These peak positions and the 2.1 eV difference between them are similar to those found in the literature [17]. The spectra for PPOFCB on copper (Fig. 6c) and for PPHFP (Fig. 6d) were assigned the same binding energy for CF_3. These two spectra do not exhibit a peak at 285 eV.

The curve fit for the PPOFCB C_{1s} spectrum in Fig. 7 was based on finding a fit that best suited the CF_3 and CF_2 peaks. These two prominent peaks are best fit using a 50% Gaussian/Lorenzian distribution and a FWHM of 1.9 eV. These two fitting parameters were then used to fit the entire spectrum, positioning peaks at 289.5 and 286.9 eV, the other maxima in the spectrum. The resulting fit indicated that a fifth peak must be added at 288.2 eV. The peaks at 289.5, 288.2 and 286.9 eV were assigned to $C^*F–CF_n$, CF and $C^*–CF_n$, respectively, in accordance with other plasma fluoropolymer XPS studies in the literature [18]. $C^*F–CF_n$ and $C^*–CF_n$ represent, respectively, monofluorinated carbon and non-fluorinated carbon affected by a neighborhood of highly fluorinated carbon. The tail of the spectrum at low binding energies results from the $\alpha_{3,4}$ satellites of the higher energy peaks. A FWHM of 1.9 eV was needed to fit the composite peaks associated with the irregular structure of the plasma polymer in Fig. 6b. A FWHM of 1.4 eV was used

Table 2
Molecular structure of plasma polymers from C_{1s} curve fit peak areas

Group	Energy[a] (eV)	Relative area, A (%)	
		PPOFCB	PPHFP
CF_3	293.5	24.2	18.3
CF_2	291.4	32.9	25.2
C^*F–CF	289.5	15.3	19.8
CF	288.2	9.9	13.7
C^*–CF	286.9	17.7	23.0
CH	285	0.0	0.0

[a] ± 0.1 eV.

to fit the PE peak at 285 eV in Fig. 6a; the PE structure does not produce the broad composite peaks associated with plasma polymers. The shoulder at 285 eV in Fig. 6b could only be fit using a FWHM of 1.4 eV. This confirms that the origin of the shoulder at 285 eV in Fig. 6b is the PE substrate and not a composite peak from the plasma polymer.

The spectrum of PPHFP in Fig. 8 was fit in the same manner. The best fit to the prominent CF_3 and CF_2 peaks occurred with a 55% Gaussian distribution, a FWHM of 2.0 eV, and peak energies that were about the same (±0.1 eV) as those found for the PPOFCB curve fit. The similarity between the C_{1s} curve fits for two plasma fluoropolymers from different monomers, in different reactors and at different powers and pressures, attests to the soundness of the curve fits. The relatively insignificant amount of oxygen bound to carbon was ignored for these curve fits.

The concentrations of CF_3, CF_2, C^*F–CF_n, CF and C^*–CF in Table 2 are based on the relative peak area, A. The total CF, ΣCF, is the sum of the CF and C^*F–CF_n in Table 2. PPOFCB had a relatively high concentration of CF_2 (32.9%), about 25% CF_3 and about 25% ΣCF. PPHFP has a relatively high concentration of ΣCF (33.5%) and smaller amounts of CF_3 and CF_2 (18.3 and 25.2%, respectively). This is not an unexpected result, given the structure of HFP and the higher W/F_m that would yield more extensive fragmentation and etching. The lower W/F_m for PPOFCB yields a polymer structure similar to that of the monomer and, therefore, richer in CF_2.

The validity of these results was confirmed by Table 3 in which the F and C contents derived from the curve fits in Table 2 are compared with those from the atomic composition analysis in Table 1. The F content was calculated from the results in Table 2 using Eq. (1), which is only applicable

Table 3
F and C contents from Tables 1 and 2

	PPOFCB		PPHFP	
	Table 1[a]	Table 2	Table 1[a]	Table 2
F (%)	60.5	62.1	60.0	58.1
C (%)	39.5	37.9	40.0	41.9

[a] Normalized to F + C = 100%.

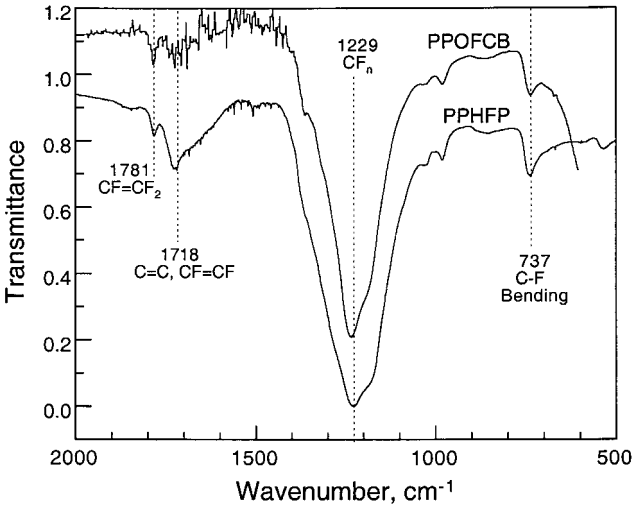

Fig. 9. FTIR spectra of PPOFCB (7 W, 10 sccm, 2.67 Pa) and HFP (100 W, 18 sccm, 187 Pa).

when all the atoms are included within the C_{1s} curve fit. An alternative equation, applicable in all cases, yields indistinguishable results. The alternative equation, which uses the experimental atomic concentrations, was used when the above assumption was not valid [14]. Eq. (1) is based solely on theory and is therefore a more sensitive test of its validity.

$$F = \frac{3A(CF_3) + 2A(CF_2) + A(CF) + A(C^*F - CF_n)}{3A(CF_3) + 2A(CF_2) + A(CF) + A(C^*F - CF_n) + 100} \times 100\% \quad (1)$$

Table 3 presents the results from Table 1 normalized to F + C = 100% (the curve fit did not take the negligible amount of oxygen into account). Table 3 shows that there is an average variation of ±2% in elemental concentrations between the results from Tables 1 and 2, well within experimental error.

The FTIR spectra of PPOFCB and PPHFP in Fig. 9 are surprisingly similar for two plasma fluoropolymers from different monomers, polymerized in different reactors and at different powers and pressures. This confirms the general similarity in molecular structure suggested by the XPS analyses. Both plasma fluoropolymers exhibit the following FTIR peaks: CF = CF_2 (1781 cm^{-1}), CF = CF (1718 cm^{-1}), CF_n (1229 cm^{-1}), and CF bending (737 cm^{-1}) [9]. The spectra can be compared by normalizing the peak heights in each spectrum to the CF_n peak height at 1229 cm^{-1}. The peak heights normalized in this fashion and the ratio of the PPHFP normalized peak heights to the PPOFCB normalized peak heights are listed in Table 4. The PPOFCB and PPHFP normalized peak heights for the peaks at 981 and 737 cm^{-1} are quite similar, with a peak ratio of about 1.0. The PPHFP normalized peak heights for the peaks at 1781 and 1718 cm^{-1}, however, are 50% larger than those for

Table 4
FTIR peak heights normalized by the 1229 cm^{-1} peak height

Wavenumber, cm^{-1}	PPOFCB	PPHFP	PPHFP/PPOFCB
1781	0.08	0.12	1.50
1718	0.16	0.24	1.50
981	0.13	0.13	1.00
737	0.14	0.15	1.07

PPOFCB. These peaks represent $CF=CF_2$ and $CF=CF$, respectively, indicating that PPHFP contains significantly more unsaturation in its structure. This significantly greater amount of unsaturation may reflect the presence of the double bond in HFP and/or enhanced fragmentation and etching at the higher W/F_m.

The molecular structures of PPOFCB and PPHFP are, at first glance, quite similar. The higher CF_2 and lower unsaturation contents, and smoother surface of PPOFCB, however, suggest that it would be a superior material for low permittivity applications. The desired F/C for PPOFCB can be achieved using less extensive fragmentation (lower W/F_m) and higher reactant concentrations (higher pressures).

3.4. Adhesion

The plasma fluoropolymers adhere strongly to substrates. Several attempts were made to quantify the adhesion of plasma polymers to copper. A Scotch Tape peel test could not debond the polymers from the substrate. Scratch tests produced the type of scratch seen in Fig. 10: note that the indentor ploughed through the polymer but could not debond it from the copper. An attempt to propagate a crack between the layers produced a failure at the Cu/Si interface, rather than at the polymer/Cu interface.

3.5. Permittivity

The PPOFCB (7 W, 24 sccm, 33.3 Pa) refractive index, determined through variable wavelength ellipsometry, is 1.37 at 900 nm. This relatively low refractive index indicates that PPOFCB is a potentially attractive low κ dielectric with a permittivity in the neighborhood of 2.0 (i.e. n^2) at high frequencies.

4. Conclusions

The plasma polymerizations of OFCB, HFP and TrFE were investigated with the objective of synthesizing a smooth fluoropolymer film with a low permittivity. These films, with their relatively high F/C ratios, were investigated in more detail. The PPOFCB refractive index of 1.37 at a wavelength of 900 nm suggests that PPOFCB has potential as a low κ dielectric with a high frequency permittivity in the neighborhood of 2.0. This investigation has shown:

- Transparent, yellow fluoropolymer films that adhere strongly to the substrates were deposited at constant deposition rates that ranged from 0.03 μm/min for PPOFCB to 0.34 μm/min for PPHFP.
- The deposition rate increases with W/F_m until a critical W/F_m of approximately 25 MJ/kg is attained. Beyond this critical W/F_m, the PPOFCB deposition rate reaches a plateau and the PPHFP deposition rate begins to decrease, reflecting an increase in etching rate.
- The roughness of PPOFCB on copper is 0.46 nm, half the 0.97 nm roughness of the substrate. The significantly rougher PPTrFE and PPHFP consist of spherical particles from a predominantly gas phase polymerization. The smoothness of the PPOFCB films would be advantageous for ILD applications.

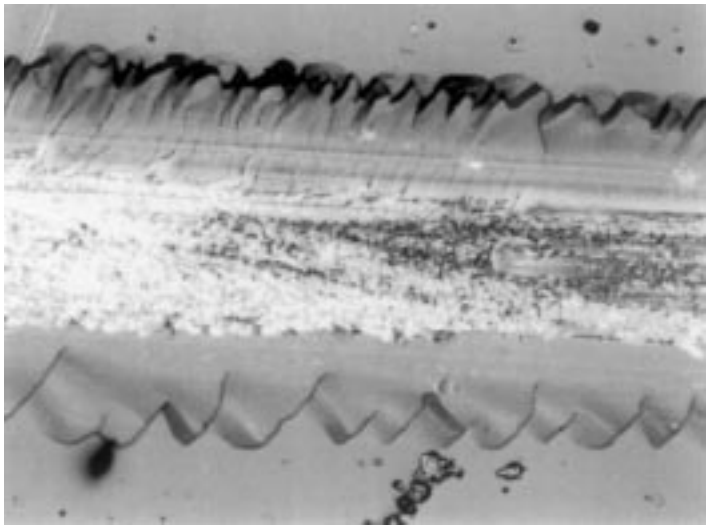

Fig. 10. Optical micrograph of scratch in PPOFCB (7 W, 10 sccm, 2.67 Pa) on copper after scratch test.

- The incorporation of fluorine in the polymer is more efficient for PPOFCB and PPHFP. The PPOFCB F/C increases with decreasing W/F_m and, in a less sensitive manner, with increasing pressure, with a typical F/C of 1.5. The approximately 1.5% oxygen results from the reaction of long-lived radicals in the plasma polymer with atmospheric oxygen.
- PPOFCB and PPHFP are similar in structure, consisting of a random assembly of fluorinated carbon groups. CF_2 groups are more prevalent in PPOFCB, while CF groups are more prevalent in PPHFP, which contains significantly more unsaturated groups than does PPOFCB.

Acknowledgements

The authors gratefully acknowledge the support of the Technion VPR Fund and the Natural Sciences and Engineering Council of Canada.

References

[1] Lee WW, Ho PS. MRS Bull 1997;22(10):28.
[2] National Technology Roadmap for Semiconductors — Technology Needs — 1998. New York: SEMATECH, 1998.
[3] Sacher E, Klemberg-Sapieha JE. J Vac Sci Technol A 1997; 15:2143.
[4] Sandrin L, Sacher E. Appl Surf Sci 1998;135:339.
[5] Popovici D, Meunier M, Sacher E. J Appl Phys 1998;83:108.
[6] Popovici D, Meunier M, Sacher E. J Appl Polym Sci 1998; 70:1201.
[7] Popovici D, Meunier M, Sacher E. J Adhes 1999;70:155.
[8] Chen R, Gorelik V, Silverstein MS. J Appl Polym Sci 1995;56: 615.
[9] Chen R, Silverstein MS. J Polym Sci A: Polym Chem 1996;34:207.
[10] Silverstein MS, Chen R, Kesler O. Polym Engng Sci 1996;36:2542.
[11] Silverstein MS, Sadovsky J, Alon D, Wahad V. J Appl Polym Sci 1999;72:405.
[12] Yasuda H. Plasma polymerization. New York: Academic Press, 1985.
[13] Morosoff N. In: d'Agostino R, editor. Plasma deposition, treatment, and etching of polymers, New York: Academic Press, 1990. p. 1.
[14] Silverstein MS, Sandrin L, Sacher E. Polymer issue in press.
[15] Sherwood PM. In: Briggs D, Seah MP, editors. Practical surface analysis by auger and X-ray photoelectron spectroscopy. New York: Wiley, 1983. p. 445.
[16] d'Agostino R. In: d'Agostino R, editor. Plasma deposition, treatment, and etching of polymers. New York: Academic Press, 1990. p. 95.
[17] Beamson G, Briggs D. High resolution XPS of organic polymers. New York: Wiley, 1992.
[18] Ryan ME, Fonseca JLC, Trasker S, Badyal JPS. J Phys Chem 1995;99:7060.